Scientific Research Publishing

Stem Cell Discovery, 2026, 16(1), 1-15
https://www.scirp.org/journal/scd
ISSN Online: 2161-6787
ISSN Print: 2161-6760

Intradermal hUC-MSC Therapy for Infraorbital Wrinkles and Nasolabial Fold Aging: Two Quantitatively Analyzed Clinical Cases

Artit Ramdongbang*, Suwimom Charoenkankar

LBM Stem Cell Research Unit, Bangkok, Thailand
Email: *lbm.mss001@gmail.com

How to cite this paper: Ramdongbang, A. and Charoenkankar, S. (2026) Intradermal hUC-MSC Therapy for Infraorbital Wrinkles and Nasolabial Fold Aging: Two Quantitatively Analyzed Clinical Cases. *Stem Cell Discovery*, **16**, 1-15.
https://doi.org/10.4236/scd.2026.161001

Received: December 30, 2025
Accepted: January 28, 2026
Published: January 31, 2026

Abstract

Age-related facial aging presents with heterogeneous clinical phenotypes, including superficial wrinkle formation and structural volume loss, reflecting distinct but interrelated changes within the dermal and subdermal layers. Current treatment approaches remain limited in their ability to address both surface texture and underlying structural deficits in a coordinated manner. In this exploratory dual-case study, we assessed the clinical and image-derived outcomes following intradermal administration of human umbilical cord-derived mesenchymal stem cells (hUC-MSCs, passage 5) combined with human placental extract (HPE) in two male patients representing different facial aging patterns: infraorbital wrinkle-dominant aging and nasolabial fold volume-loss-dominant aging. Standardized clinical photographs were obtained at baseline (Month 0) and at Months 1 - 3 under controlled imaging conditions. Quantitative analysis was performed using ImageJ with predefined regions of interest. Relative surface parameters were derived from grayscale mapping, line-profile analysis, and surface roughness measurements. In the infraorbital case, reductions in relative wrinkle depth index, surface roughness, and wrinkle area fraction were observed over the follow-up period, accompanied by visible smoothing of the skin surface. In the nasolabial fold case, analysis demonstrated a progressive decrease in relative fold depth index and peak-to-valley amplitude, consistent with gradual improvement in contour profile rather than an immediate filling effect. No serious adverse events were reported. Mild transient edema occurred and resolved within 48 hours without intervention. Overall, both cases demonstrated consistent directional changes in quantitative metrics and corresponding clinical appearance over time. These findings suggest that combined hUC-MSC and HPE administration may contribute to gradual dermal remodeling and improvement in facial contour. However, interpretation is limited by the small sample size and the use of two-dimensional image-

based measurements. Further controlled studies incorporating objective three-dimensional assessment are required to validate these observations and clarify underlying mechanisms.

Keywords

Human Placental Extract (HPE), Mesenchymal Stem Cells (MSCs), Cell Proliferation, Cell Differentiation, Activity, Regenerative Medicine, Placental Biomaterials, Cell Adhesion

1. Introduction

Facial aging is a complex, progressive biological process involving cumulative alterations in dermal cellularity, extracellular matrix (ECM) organization, and subcutaneous soft tissue architecture. At the microscopic level, aging skin exhibits reduced fibroblast activity, collagen fragmentation, elastin disorganization, and impaired ECM turnover, which collectively manifest clinically as fine and static wrinkles, surface roughness, and loss of facial contour continuity [1]-[3]. Importantly, these changes reflect diminished regenerative capacity rather than isolated structural defects. Current aesthetic interventions predominantly focus on symptomatic correction. Dermal fillers provide immediate volume replacement, while energy-based devices induce controlled tissue injury to stimulate secondary repair responses. Although effective for short-term cosmetic improvement, these approaches do not directly address the underlying biological dysregulation of tissue homeostasis and may offer limited durability in the absence of sustained regenerative signaling [4] [5]. Mesenchymal stem cells (MSCs) have emerged as promising candidates for regenerative therapies due to their capacity to modulate tissue repair through paracrine mechanisms rather than direct differentiation [6]-[8]. Increasing evidence indicates that MSCs exert their biological effects primarily via secretion of bioactive factors, including cytokines, growth factors, and extracellular vesicles such as exosomes, which collectively influence fibroblast activity, angiogenesis, immune modulation, and ECM remodeling [6] [9]-[11]. This paracrine paradigm aligns closely with the pathophysiology of skin aging, where restoration of cellular signaling and matrix dynamics is required for meaningful rejuvenation [2] [10]. Among various MSC sources, human umbilical cord-derived MSCs (hUC-MSCs) demonstrate several advantages, including high proliferative capacity, low immunogenicity, and relatively stable phenotypic characteristics when expanded under Good Manufacturing Practice (GMP) conditions [11]-[16]. Previous studies have demonstrated that Wharton's jelly-derived MSCs exhibit favorable proliferative behavior and immunomodulatory properties compared with several adult tissue sources [15] [17] [18]. Importantly, hUC-MSCs have been shown to exhibit robust secretory profiles enriched in ECM-regulatory and anti-inflammatory mediators, suggesting potential utility in skin regeneration and soft tissue remodeling [3] [19]-[21]. Exosomes derived from MSCs have gained

particular attention as key mediators of regenerative signaling. These nanoscale vesicles transport functional proteins, lipids, and microRNAs that regulate fibroblast proliferation, collagen synthesis, and matrix metalloproteinase activity, thereby influencing ECM architecture and tissue mechanical properties [1]-[3] [9]. Rather than inducing abrupt structural changes, exosome-mediated effects are typically gradual and spatially distributed, consistent with biological remodeling processes [10]. Human placental extract (HPE) contains a complex mixture of peptides, growth factors, and matrix-associated molecules that may support cellular communication and ECM homeostasis [21] [22]. Several placental-associated growth factors, including PDGF, VEGF, and PlGF signaling pathways, have been implicated in angiogenesis, wound healing, and tissue remodeling processes [23]-[28]. In addition, growth factor-dependent modulation of mesenchymal cell differentiation and survival has been demonstrated in multiple experimental systems [29]-[31]. When administered in conjunction with MSCs, HPE may act as a permissive microenvironmental modulator, potentially enhancing MSC paracrine signaling and sustaining regenerative cascades. However, clinical data describing the combined use of MSCs and HPE for facial rejuvenation remain limited, particularly with respect to objective, quantitative outcome assessment [10] [32]. A major challenge in regenerative aesthetic research lies in the objective evaluation of treatment outcomes. While advanced three-dimensional volumetric imaging provides precise measurements, such technologies are not always accessible or practical in early-stage clinical investigations. Image-based analytical platforms, including ImageJ, offer a pragmatic alternative for longitudinal surface topology analysis. When applied conservatively and within standardized regions of interest, these methods allow relative quantification of surface depth, roughness, and contour changes over time, complementing qualitative clinical assessment [10]. In the present report, we describe two cases treated with intradermal administration of GMP-expanded hUC-MSCs (passage 5) combined with human placental extract. The cases represent distinct facial aging phenotypes: wrinkle-dominant infraorbital aging and volume-loss-dominant cheek hollowing. By integrating blinded clinical evaluation with ImageJ-based quantitative surface analysis, this study aims to provide structured documentation of phenotype-specific regenerative responses and to explore the potential role of MSC-exosome-ECM interactions in facial rejuvenation [33]-[36].

2. Materials and Methods

2.1. Ethical Considerations

Umbilical cord tissue and placental tissue were obtained from a single healthy donor following written informed consent from the mother prior to delivery. All procedures were conducted in accordance with institutional ethical guidelines and the principles of the Declaration of Helsinki. Donor screening was performed and confirmed negative for HIV-1/2, hepatitis B virus (HBV), hepatitis C virus (HCV), and syphilis.

2.2. Placenta Extraction

Placental fragments were repeatedly rinsed with a 0.15 M sodium chloride (NaCl) solution until mucus and blood were visibly removed. The fetal membranes, including the amniotic and chorionic layers, were then separated. Next, a thin layer of the cotyledon area was cut into small pieces. These pieces were mixed with physiological saline at a 1:5 weight ratio and stirred for 2 - 3 minutes. The supernatant was discarded, and fresh physiological saline was added, repeating the process 3 - 4 times. The washed placenta fragments were homogenized using a homogenizer, with the addition of physiological saline solution at a 1:1 (v/v) ratio. Soak the placenta for 12 hours, followed by centrifugation at 3000 rpm for 8 minutes. The supernatant was collected and filtered through a 0.45 μm membrane filter (Millipore Corp; Cork, Ireland). The resulting filtrate, which was an aqueous-saline HPE, was then divided into aliquots for further analysis [7] [20].

2.3. Cell Culture and Preparation

Umbilical cord tissue was processed under sterile conditions. The tissue was rinsed with phosphate-buffered saline (PBS) to remove residual blood, and umbilical arteries and veins were carefully removed. The remaining Wharton's jelly was dissected and cut into small fragments (approximately 1 - 3 mm^3) using sterile surgical instruments. The tissue fragments were plated in T75 culture flasks and maintained in α-modified Eagle medium (α-MEM) supplemented with 10% fetal bovine serum (FBS) and 1% penicillin-streptomycin. Cultures were incubated at 37˚C in a humidified atmosphere containing 5% CO_2. Medium was replaced every 2 - 3 days until adherent fibroblast-like cells migrated from the explants and reached approximately 80% confluence. Cells were passaged using 0.25% trypsin-EDTA and expanded up to passage 5 for further characterization and clinical application [15] [16] [27] [35] [37]. Immunophenotypic characterization was performed by flow cytometry in accordance with the criteria defined by the International Society for Cellular Therapy [23]. Briefly, cells were harvested and resuspended in PBS, followed by incubation with fluorochrome-conjugated antibodies against CD73, CD90, CD105, CD34, CD45, CD14, CD19, and HLA-DR. Appropriate isotype controls were included to assess nonspecific staining. After incubation, cells were washed and analyzed using a flow cytometer (BD Biosciences), and data were processed using CellQuest Pro software. Prior to clinical use, cells were evaluated for viability, sterility, mycoplasma contamination, endotoxin levels, and karyotype stability as described in subsequent sections [18] [21] [22].

For administration, cells at passage 5 were harvested at approximately 80% confluence, centrifuged to obtain a cell pellet, and resuspended in sterile 0.9% normal saline solution (NSS). The final preparation contained 1.0×10^7 cells in a total volume of 2.0 mL, combined with human placental extract (HPE) at a defined concentration. The cell suspension was prepared immediately prior to intradermal injection.

2.4. Karyotyping Assay

Karyotyping assay Proliferating MSCs were treated with colcemid at a concentration of 0.10 lg/mL for 3 h. Primary cells were harvested, and then used for karyotyping as previously published. Briefly, a single cell suspension was incubated in hypotonic solution for 30 min at 37˚C, and then fixed at least 3 times in Carnoy's solution, which included an overnight fixative step. The fixed cell suspension was dropped on wellprepared slides and stained according to the G-Banding protocol. Sets of chromosomes were analyzed using Ikaros software (MetaSystems, Altlussheim, Germany) [35] [38].

2.5. Patient History and Case Description

Two male patients presenting with distinct facial aging phenotypes were included in this study. Both patients provided written informed consent prior to treatment, and all procedures were conducted in accordance with institutional ethical guidelines. For both cases, intradermal administration of human umbilical cord-derived mesenchymal stem cells (hUC-MSCs, passage 5) was performed under sterile conditions. Cells were prepared as described in Section 2.3 and resuspended in sterile 0.9% normal saline solution (NSS) at a final dose of 1.0×10^7 cells in 2.0 mL, combined with human placental extract (HPE). Injections were performed using a 30G needle via a microdroplet technique at the intradermal to superficial subdermal plane. Approximately 20 - 30 injection points were distributed across the treatment area with spacing of approximately 1 cm. Topical 5% lidocaine was applied prior to the procedure. Patients were instructed to avoid ultraviolet exposure and additional aesthetic procedures during the follow-up period.

Case 1

A 42-year-old male presented with concerns regarding progressive periocular aging, predominantly fine static wrinkles and early crow's feet in the infraorbital region. The patient reported gradual worsening over several years, characterized by reduced skin smoothness and increased wrinkle visibility during neutral facial expression. No prior aesthetic procedures, including dermal fillers, botulinum toxin, or energy-based devices, had been performed in the periocular area. The patient was otherwise healthy, with no history of autoimmune disease, chronic inflammatory conditions, bleeding disorders, or known hypersensitivity reactions. He was a nonsmoker and denied regular use of systemic corticosteroids or immunomodulatory medications. Skin type was classified as Fitzpatrick type III. Baseline clinical examination revealed mild-to-moderate static infraorbital wrinkles without significant volume loss, edema, or pigmentation abnormalities. The primary treatment objective was regenerative skin rejuvenation rather than volumetric augmentation. The patient received intradermal administration of hUC-MSCs (passage 5) prepared under controlled conditions, as described above.

Case 2

A 47-year-old male presented with a primary complaint of progressive deepening of the nasolabial folds, associated with midfacial volume loss and reduced con-

tour support along the nasolabial-malar interface. The patient reported gradual worsening of nasolabial crease depth over the preceding 5 - 7 years, resulting in increased shadowing and a more aged facial appearance, particularly during static facial expression. He denied any history of facial trauma, connective tissue disease, or prior facial surgical procedures. The patient had not previously received dermal fillers, fat grafting, or stem cell-based therapies, and reported only intermittent use of topical anti-aging products with minimal perceived benefit. His medical history was otherwise unremarkable, and no contraindications to regenerative intervention were identified. Fitzpatrick skin type was classified as type IV. Baseline clinical examination demonstrated moderate-to-severe nasolabial fold depth with a well-defined crease extending from the alar base toward the oral commissure. The contour abnormality was characterized predominantly by structural soft tissue depletion and loss of midfacial support rather than superficial dermal wrinkling. Skin texture overlying the nasolabial region appeared relatively preserved, while the fold depth and shadowing were accentuated by underlying volume deficiency. Given the patient's preference to avoid synthetic volumizing fillers and to pursue a gradual, biologically mediated approach to facial rejuvenation, intradermal administration of hUC-MSCs (passage 5) in combination with HPE was selected. The therapeutic goal was to induce progressive dermal-subdermal remodeling and structural support restoration rather than immediate volumetric correction.

2.6. ImageJ-Based Image Analysis

Standardized clinical photographs were obtained at baseline (Day 0; Month 0) and at follow-up visits corresponding to Day 30 (Month 1), Day 60 (Month 2), and Day 90 (Month 3). All images were captured under consistent lighting conditions, camera settings, and patient positioning. Images were aligned using fixed anatomical landmarks to ensure spatial consistency across time points. Quantitative image analysis was performed using ImageJ (National Institutes of Health, USA). For surface visualization, grayscale-derived height maps were generated using the ImageJ 3D Surface Plot plugin. Regions of interest (ROIs) corresponding to the infraorbital wrinkle area and nasolabial fold were manually delineated in a blinded manner. Surface roughness parameters, including mean surface height variation and peak-to-valley amplitude, were extracted using line-profile analysis to assess temporal changes in skin surface characteristics. Given that analysis was performed on two-dimensional photographic data, all reported "depth" values represent relative image-derived indices rather than absolute physical measurements. Accordingly, results are interpreted based on relative changes over time rather than true dimensional depth. All measurements were performed in triplicate for each time point, and results are presented as mean ± standard deviation to illustrate longitudinal trends within each case.

2.7. Statistical Analysis

Given the exploratory nature of this study and the limited sample size (n = 2), clin-

ical outcomes were analyzed descriptively. Data are presented as mean ± standard deviation and percentage change from baseline. Inferential statistical analysis (two-way ANOVA and Tukey post hoc test) was applied only to *in vitro* experiments evaluating the effects of HPE on MSC growth (n = 3 independent replicates per condition). A p-value < 0.05 was considered statistically significant.

3. Result

3.1. Immunophenotypic Characterization of hUC-MSCs

Flow cytometric analysis was performed to characterize the immunophenotypic profile of the isolated cells in accordance with the criteria established by the International Society for Cellular Therapy (ISCT) [11] [23]. A standardized gating strategy was applied, including exclusion of debris based on forward and side scatter properties, doublet discrimination, and viability gating prior to marker analysis. The analyzed cell population demonstrated a homogeneous mesenchymal stem cell phenotype. High expression of MSC-associated surface markers was observed, with CD73 (99.2% ± 0.4%), CD90 (99.5% ± 0.3%), and CD105 (98.8% ± 0.5%) consistently expressed across the majority of the cell population. In contrast, expression of hematopoietic and immune lineage markers, including CD34 (0.6%), CD45 (0.4%), CD14 (0.3%), CD19 (0.2%), and human leukocyte antigen-DR (HLA-DR; 0.5%), remained minimal and consistently below 1%. Cell viability at the time of analysis exceeded 90%, confirming the integrity of the analyzed population. These findings confirm that the isolated and expanded hUC-MSCs met the minimal immunophenotypic criteria defined by the ISCT and exhibited a high degree of cellular purity, supporting their suitability for subsequent experimental and clinical application [15] [18] [23] [27] [37].

3.2. Effects of Human Placental Extract on MSC Growth and Adhesion

The growth behavior of human umbilical cord-derived mesenchymal stem cells (hUC-MSCs) cultured in the presence of human placental extract (HPE) was evaluated over a 21-day period using quantitative cell counting and morphological assessment. HPE concentrations were expressed as protein-equivalent values (0.02, 0.05, 0.1, 0.15, and 0.2 μg/mL). Across all conditions, MSCs exhibited a time-dependent increase in cell number. Higher HPE concentrations were generally associated with greater cell expansion. At Day 21, the highest cell density was observed at 0.2 μg/mL HPE (12.24×10^6 cells/75cm^2), whereas the lowest value was recorded at 0.02 μg/mL on Day 7 (0.68×10^6 cells/75cm^2). Cells cultured with 0.15 μg/mL HPE reached 10.06×10^6 cells/75cm^2 by Day 21, exceeding the corresponding control condition. Linear regression analysis demonstrated a consistent positive relationship between culture duration and cell growth across all HPE concentrations, with coefficients of determination (R^2) ranging from 0.9006 to 0.9636. The highest correlation was observed at 0.2 μg/mL ($R^2 = 0.9636$), indicating stable expansion under this condition.

Fluorescence staining with DAPI and rhodamine-phalloidin was performed at Days 0, 7, 14, and 21 to assess nuclear morphology and cytoskeletal organization across different HPE concentrations. Distinct nuclear staining and organized F-actin structures were observed in all conditions throughout the culture period. Cells exhibited a flattened, fibroblast-like morphology with evident lamellipodial extensions, consistent with adherent mesenchymal cell characteristics. Cell coverage increased progressively over time across all conditions, with a more pronounced increase observed at higher HPE concentrations. At later time points, particularly at Day 21, cultures treated with higher concentrations, including 0.15 μg/mL (150 pg/mL) and 0.2 μg/mL (200 pg/mL) HPE, showed greater cell density compared to lower concentrations, consistent with the growth kinetics presented in Figure 1. Quantitative analysis of DAPI-stained nuclei using ImageJ demonstrated a time-dependent increase in cell density across all HPE concentrations. The highest cell density was consistently observed at 0.2 μg/mL (200 pg/mL) HPE, in agreement with the growth curve data. The increase in cell number occurred progressively over the culture period without abrupt changes in growth pattern. Taken together, the morphological observations and quantitative analysis are consistent with a concentration-dependent increase in MSC expansion under HPE supplementation over the 21-day culture period.

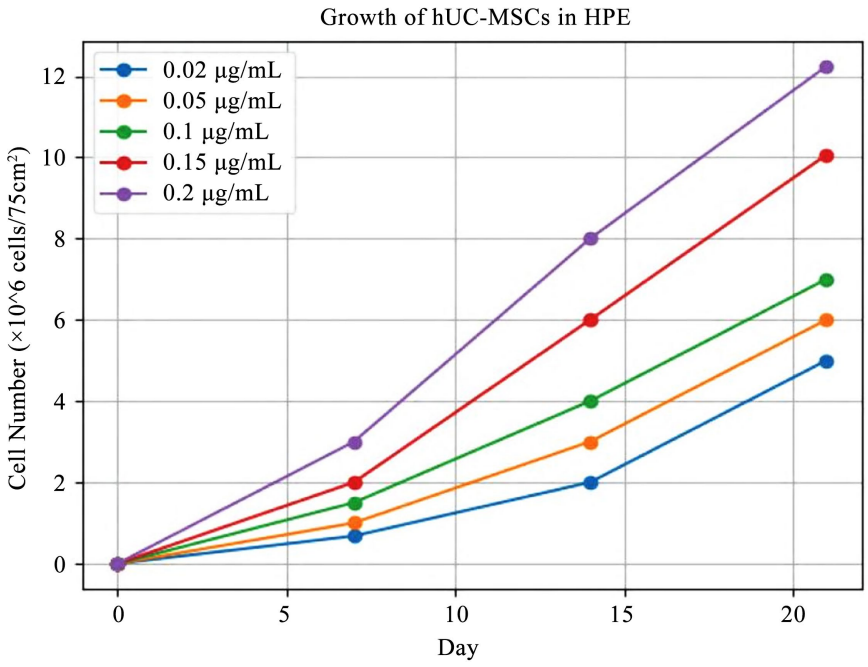

Figure 1. Growth kinetics of human umbilical cord-derived mesenchymal stem cells (hUC-MSCs) cultured with human placental extract (HPE). Cells were cultured for 21 days in the presence of HPE at concentrations of 0.02, 0.05, 0.1, 0.15, and 0.2 μg/mL (20, 50, 100, 150, and 200 pg/mL). Cell density ($\times 10^6$ cells per 75 cm^2) was measured at indicated time points and plotted against culture duration. A time-dependent increase in cell number was observed across all conditions, with higher HPE concentrations associated with greater cell expansion. Linear regression analysis demonstrated a positive correlation between culture duration and cell growth (R^2 = 0.9006 - 0.9636).

3.3. ImageJ-Based 3D Quantitative Assessment

Case 1: Infraorbital wrinkle-dominant phenotype

Case 1 presented with moderate static infraorbital wrinkles without prominent volume deficiency at baseline (Month 0) (Figure 2). Quantitative image analysis was performed on standardized clinical photographs using ImageJ, with a predefined region of interest (ROI) encompassing the infraorbital area. Wrinkle morphology was evaluated using surface roughness parameters derived from grayscale height mapping and line-profile analysis. At baseline (Month 0), the mean wrinkle depth within the ROI was measured at 182.6 ± 14.3 μm, with a wrinkle surface roughness (Ra) value of 41.8 ± 3.9 arbitrary units (a.u.) and a wrinkle area fraction of 22.4%, as summarized in Table 1(a). By Month 1 following intradermal administration of hUC-MSCs (passage 5) in combination with human placental extract (HPE), a modest reduction in wrinkle depth was observed, with mean depth decreasing to 156.4 ± 12.7 μm, corresponding to a 14.4% reduction from baseline. Surface roughness similarly decreased to 35.2 ± 3.1 a.u. (−15.8%), while wrinkle area fraction declined to 16.1%, indicating early improvement in infraorbital skin texture and wrinkle morphology (Table 1(a)).

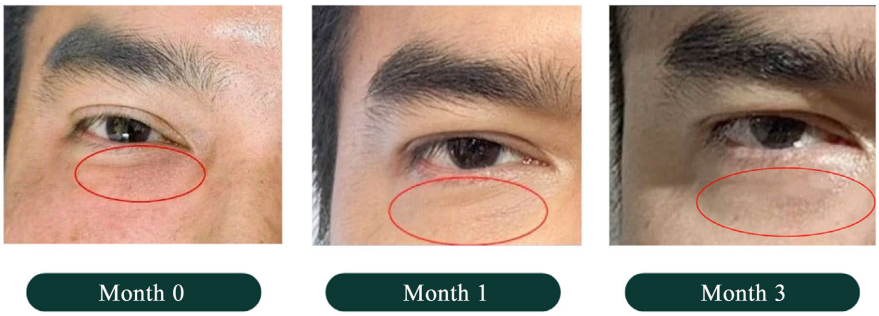

Figure 2. Serial clinical images and ImageJ-based quantitative analysis of infraorbital wrinkle remodeling in Case 1.

Table 1. ImageJ-derived quantitative outcomes for Case 1 and Case 2 over 3-month follow-up. (a) Case 1: Infraorbital wrinkle-dominant phenotype; (b) Case 2: Nasolabial fold dominant volume loss phenotype.

(a)

Time point	Mean wrinkle depth (μm)	% change vs Baseline	Surface roughness Ra (a.u.)	% change vs baseline	Wrinkle area fraction (%)
Month 0	182.6 ± 14.3	0%	41.8 ± 3.9	0%	22.4
Month 1	156.4 ± 12.7	−14.4%	35.2 ± 3.1	−15.8%	16.1
Month 3	118.9 ± 11.6	−34.9%	27.6 ± 2.8	−33.9%	11.8

(b)

Time point	Mean nasolabial fold depth (mm)	% change vs baseline
Month 0	2.84 ± 0.21	0%
Month 1	2.31 ± 0.19	−18.7%
Month 3	1.61 ± 0.15	−43.3%

At Month 3, further improvement was evident. Mean wrinkle depth was reduced to 118.9 ± 11.6 μm, representing an overall reduction of 34.9% relative to baseline, whereas surface roughness declined to 27.6 ± 2.8 a.u., corresponding to a 33.9% decrease (Table 1(a)). In parallel, wrinkle area fraction further decreased to 11.8%, reflecting progressive reduction in wrinkle burden within the analyzed ROI. Line-profile analysis demonstrated a visible reduction in peak-to-valley amplitude and a smoothing of wrinkle contours across the infraorbital surface. Three-dimensional surface reconstruction suggested progressive flattening of the infraorbital microtopography over time, with a reduction in maximal depression depth and improved continuity of the dermal surface (Figure 2). The temporal pattern of change was gradual and progressive across the 3-month follow-up period, consistent with tissue remodeling rather than an immediate volumetric filling effect, as quantitatively demonstrated in Table 1(a).

Case 2: Infraorbital volume-loss-dominant phenotype

Case 2 exhibited a volume-loss-dominant aging phenotype primarily involving the nasolabial fold, characterized by a pronounced and deepened fold extending from the alar base toward the oral commissure at baseline (Month 0) (Figure 3). No prominent infraorbital wrinkling or periorbital surface irregularity was observed, indicating that the aesthetic concern was predominantly related to midfacial volume deficiency rather than superficial textural changes. Quantitative image analysis was performed on standardized frontal and oblique facial photographs using ImageJ. A predefined region of interest (ROI) was delineated along the nasolabial fold, encompassing the area of maximal concavity. Fold depth and contour geometry were assessed using grayscale intensity profiling and line-profile analysis perpendicular to the fold axis.

Figure 3. Representative frontal and oblique views of Case 2 at baseline (Month 0) and Month 3 after intradermal administration of hUC-MSCs (P5) combined with HPE. The highlighted regions correspond to the nasolabial fold ROI analyzed using ImageJ, demonstrating concordant qualitative visual improvement and quantitative reduction in fold depth over time.

At baseline, the mean nasolabial fold depth within the ROI measured 2.84 ± 0.21 mm, with a high peak-to-valley amplitude reflecting marked contour depression, as shown in Table 1(b). Following intradermal administration of hUC-MSCs (passage 5) in combination with human placental extract (HPE), progressive vol-

umetric improvement was observed over time. At Month 1, mean fold depth decreased to 2.31 ± 0.19 mm, corresponding to an 18.7% reduction relative to baseline (Table 1(b)). By Month 3, further improvement was evident, with fold depth reduced to 1.61 ± 0.15 mm, representing an overall reduction of 43.3% from baseline values (Table 1(b)). Line-profile analysis demonstrated a gradual attenuation of the peak-to-valley amplitude and a smoothing of the nasolabial contour, with improved continuity between the midcheek and perioral regions. Three-dimensional surface reconstruction suggested restoration of midfacial convexity rather than superficial filling, with a broader and more anatomically integrated volume distribution along the nasolabial fold (Figure 3). The temporal pattern of improvement was progressive and sustained throughout the follow-up period, consistent with biologically mediated tissue regeneration and extracellular matrix remodeling rather than an immediate space-occupying effect. These findings, together with the quantitative reductions summarized in Table 1(b), support a regenerative volumizing role of combined hUC-MSC and HPE therapy in nasolabial fold-dominant facial aging.

Quantitative outcomes derived from ImageJ analysis of standardized clinical photographs in two distinct facial aging phenotypes. Case 1 demonstrated progressive reduction in infraorbital wrinkle depth, surface roughness, and wrinkle area fraction, indicating gradual dermal surface remodeling. Case 2 exhibited sustained reduction in nasolabial fold depth, consistent with biologically mediated volumetric restoration rather than immediate filling effects. Improvements in both cases followed a progressive temporal pattern over the 3-month follow-up period.

4. Discussion and Conclusion

This dual-case analysis evaluated the clinical and image-derived outcomes following intradermal administration of human umbilical cord-derived mesenchymal stem cells (hUC-MSCs) in combination with human placental extract (HPE) across two distinct facial aging phenotypes. The findings demonstrate consistent, time-dependent improvements in both wrinkle-dominant and volume-loss-dominant presentations, as assessed by standardized image analysis. In the infraorbital wrinkle-dominant case, progressive reductions in relative wrinkle depth, surface roughness, and wrinkle area fraction were observed over the 3-month follow-up period. These changes were accompanied by visible smoothing of the skin surface. In the nasolabial fold-dominant case, a gradual decrease in relative fold depth index and peak-to-valley amplitude was observed, suggesting improvement in contour distribution over time. The temporal pattern of change in both cases was gradual rather than immediate, consistent with a progressive remodeling process, which aligns with previous reports describing MSC-mediated tissue repair through paracrine signaling and extracellular vesicle activity rather than direct structural replacement [1]-[3] [6] [7] [19] [25]. The *in vitro* findings further support these observations. hUC-MSCs cultured in the presence of HPE demonstrated a concentration-dependent increase in cell expansion over a 21-day period, with stable growth kinet-

ics across all tested concentrations. Morphological assessment showed preserved cytoskeletal organization and adherent cell characteristics, consistent with sustained cell expansion under the conditions tested. Similar proliferative and regenerative-supportive properties have previously been reported in placental and umbilical cord-derived MSC systems [11] [15] [27]-[29] [32] [36]. While these findings are not directly translatable to *in vivo* mechanisms, they provide supportive context for the observed clinical trends. The mechanism underlying the observed effects was not directly investigated in this study. Therefore, proposed pathways, including paracrine signaling, extracellular matrix remodeling, angiogenic modulation, or exosome-mediated effects, should be considered hypothetical [1]-[3] [7] [12] [16] [17] [19] [25] [31]. In conclusion, intradermal administration of hUC-MSCs in combination with HPE was associated with progressive improvements in image-derived parameters across two distinct facial aging phenotypes over a 3-month period. These findings support the feasibility of this approach as a regenerative strategy; however, further controlled studies incorporating larger sample sizes and objective three-dimensional assessments are required to confirm efficacy and clarify underlying mechanisms [4] [8] [12] [25].

Conflicts of Interest

The authors declare no conflicts of interest regarding the publication of this paper.

References

[1] Hu, J.C., Zheng, C.X., Sui, B.D., Liu, W.J. and Jin, Y. (2022) Mesenchymal Stem Cell-Derived Exosomes: A Novel and Potential Remedy for Cutaneous Wound Healing and Regeneration. *World Journal of Stem Cells*, **14**, 318-329. https://doi.org/10.4252/wjsc.v14.i5.318

[2] Kim, Y., Yoo, S.M., Park, H.H., Lim, H.J., Kim, Y., Lee, S., *et al.* (2017) Exosomes Derived from Human Umbilical Cord Blood Mesenchymal Stem Cells Stimulates Rejuvenation of Human Skin. *Biochemical and Biophysical Research Communications*, **493**, 1102-1108. https://doi.org/10.1016/j.bbrc.2017.09.056

[3] Zhang, S., Chuah, S.J., Lai, R.C., Hui, J.H.P., Lim, S.K. and Toh, W.S. (2018) MSC Exosomes Mediate Cartilage Repair by Enhancing Proliferation, Attenuating Apoptosis and Modulating Immune Reactivity. *Biomaterials*, **156**, 16-27. https://doi.org/10.1016/j.biomaterials.2017.11.028

[4] Nowacki, M., Kloskowski, T., Pietkun, K., Zegarski, M., Pokrywczyńska, M., Habib, S.L., *et al.* (2017) The Use of Stem Cells in Aesthetic Dermatology and Plastic Surgery Procedures. A Compact Review of Experimental and Clinical Applications. *Advances in Dermatology and Allergology*, **34**, 526-534. https://doi.org/10.5114/ada.2017.72456

[5] Surowiecka, A. and Strużyna, J. (2022) Adipose-Derived Stem Cells for Facial Rejuvenation. *Journal of Personalized Medicine*, **12**, Article 117. https://doi.org/10.3390/jpm12010117

[6] Chen, L., Tredget, E.E., Wu, P.Y.G. and Wu, Y. (2008) Paracrine Factors of Mesenchymal Stem Cells Recruit Macrophages and Endothelial Lineage Cells and Enhance Wound Healing. *PLOS ONE*, **3**, e1886. https://doi.org/10.1371/journal.pone.0001886

[7] Domaszewska-Szostek, A., Krzyżanowska, M., Polak, A. and Puzianowska-Kuźnicka,

M. (2025) Effectiveness of Extracellular Vesicle Application in Skin Aging Treatment and Regeneration: Do We Have Enough Evidence from Clinical Trials? *International Journal of Molecular Sciences*, **26**, Article 2354. https://doi.org/10.3390/ijms26052354

[8] Tsai, P.C., Fu, T.W., Chen, Y.M.A., Ko, T.L., Chen, T.H., Shih, Y.H., *et al.* (2009) The Therapeutic Potential of Human Umbilical Mesenchymal Stem Cells from Wharton's Jelly in the Treatment of Rat Liver Fibrosis. *Liver Transplantation*, **15**, 484-495. https://doi.org/10.1002/lt.21715

[9] Batsali, A.K., Kastrinaki, M.A., Papadaki, H. and Pontikoglou, C. (2013) Mesenchymal Stem Cells Derived from Wharton's Jelly of the Umbilical Cord: Biological Properties and Emerging Clinical Applications. *Current Stem Cell Research & Therapy*, **8**, 144-155. https://doi.org/10.2174/1574888x11308020005

[10] Hass, R., Kasper, C., Böhm, S. and Jacobs, R. (2011) Different Populations and Sources of Human Mesenchymal Stem Cells (MSC): A Comparison of Adult and Neonatal Tissue-Derived MSC. *Cell Communication and Signaling*, **9**, Article 12. https://doi.org/10.1186/1478-811x-9-12

[11] Dominici, M., Le Blanc, K., Mueller, I., Slaper-Cortenbach, I., Marini, F.C., Krause, D.S., *et al.* (2006) Minimal Criteria for Defining Multipotent Mesenchymal Stromal Cells. The International Society for Cellular Therapy Position Statement. *Cytotherapy*, **8**, 315-317. https://doi.org/10.1080/14653240600855905

[12] Hong, J.W., Lee, W.J., Hahn, S.B., Kim, B.J. and Lew, D.H. (2010) The Effect of Human Placenta Extract in a Wound Healing Model. *Annals of Plastic Surgery*, **65**, 96-100. https://doi.org/10.1097/sap.0b013e3181b0bb67

[13] Ospina, J.A.G., Martinez, E.M.M., Sampa, S.H., Gomez, J.S., Palacios, M. and Barrera-Ocampo, A.A. (2026) Proteomic Profiling and Regenerative Potential of Bovine Placental Extract in Wound Healing Models. *Journal of Advanced Pharmaceutical Technology & Research*, **17**, 71-77. https://doi.org/10.4103/japtr.japtr_157_25

[14] In't Anker, P.S., Scherjon, S.A., Kleijburg-van der Keur, C., de Groot-Swings, G.M.J.S., Claas, F.H.J., Fibbe, W.E., *et al.* (2004) Isolation of Mesenchymal Stem Cells of Fetal or Maternal Origin from Human Placenta. *Stem Cells*, **22**, 1338-1345. https://doi.org/10.1634/stemcells.2004-0058

[15] Hoch, R.V. and Soriano, P. (2003) Roles of PDGF in Animal Development. *Development*, **130**, 4769-4784. https://doi.org/10.1242/dev.00721

[16] Joukov, V., Pajusola, K., Kaipainen, A., Chilov, D., Lahtinen, I., Kukk, E., *et al.* (1996) A Novel Vascular Endothelial Growth Factor, VEGF-C, Is a Ligand for the Flt4 (VEGFR-3) and KDR (VEGFR-2) Receptor Tyrosine Kinases. *EMBO Journal*, **15**, 290-298. https://doi.org/10.1002/j.1460-2075.1996.tb00359.x

[17] Hauser, S. and Weich, H.A. (1993) A Heparin-Binding Form of Placenta Growth Factor (PlGF-2) Is Expressed in Human Umbilical Vein Endothelial Cells and in Placenta. *Growth Factors*, **9**, 259-268. https://doi.org/10.3109/08977199308991586

[18] Ataliotis, P., Symes, K., Chou, M.M., Ho, L. and Mercola, M. (1995) PDGF Signalling Is Required for Gastrulation of xenopus Laevis. *Development*, **121**, 3099-3110. https://doi.org/10.1242/dev.121.9.3099

[19] Barres, B.A., Hart, I.K., Coles, H.S.R., Burne, J.F., Voyvodic, J.T., Richardson, W.D., *et al.* (1992) Cell Death and Control of Cell Survival in the Oligodendrocyte Lineage. *Cell*, **70**, 31-46. https://doi.org/10.1016/0092-8674(92)90531-g

[20] Chamberlain, G., Fox, J., Ashton, B. and Middleton, J. (2007) Concise Review: Mesenchymal Stem Cells: Their Phenotype, Differentiation Capacity, Immunological Features,

and Potential for Homing. *Stem Cells*, **25**, 2739-2749. https://doi.org/10.1634/stemcells.2007-0197

[21] Crisan, M., Yap, S., Casteilla, L., Chen, C., Corselli, M., Park, T.S., *et al.* (2008) A Perivascular Origin for Mesenchymal Stem Cells in Multiple Human Organs. *Cell Stem Cell*, **3**, 301-313. https://doi.org/10.1016/j.stem.2008.07.003

[22] da Silva Meirelles, L., Chagastelles, P.C. and Nardi, N.B. (2006) Mesenchymal Stem Cells Reside in Virtually All Post-Natal Organs and Tissues. *Journal of Cell Science*, **119**, 2204-2213. https://doi.org/10.1242/jcs.02932

[23] Bieback, K., Kern, S., Klüter, H. and Eichler, H. (2004) Critical Parameters for the Isolation of Mesenchymal Stem Cells from Umbilical Cord Blood. *Stem Cells*, **22**, 625-634. https://doi.org/10.1634/stemcells.22-4-625

[24] Kita, K., Gauglitz, G.G., Phan, T.T., Herndon, D.N. and Jeschke, M.G. (2010) Isolation and Characterization of Mesenchymal Stem Cells from the Sub-Amniotic Human Umbilical Cord Lining Membrane. *Stem Cells and Development*, **19**, 491-502. https://doi.org/10.1089/scd.2009.0192

[25] Kratchmarova, I., Blagoev, B., Haack-Sorensen, M., Kassem, M. and Mann, M. (2005) Mechanism of Divergent Growth Factor Effects in Mesenchymal Stem Cell Differentiation. *Science*, **308**, 1472-1477. https://doi.org/10.1126/science.1107627

[26] Jeschke, M.G. and Gauglitz, G.G. (2011) Umbilical Cord Lining Membrane and Wharton's Jelly-Derived Mesenchymal Stem Cells: The Similarities and Differences. *The Open Tissue Engineering and Regenerative Medicine Journal*, **4**, 21-27. https://doi.org/10.2174/1875043501104010021

[27] Gao, F., Chiu, S.M., Motan, D.A.L., Zhang, Z., Chen, L., Ji, H., *et al.* (2016) Mesenchymal Stem Cells and Immunomodulation: Current Status and Future Prospects. *Cell Death & Disease*, **7**, e2062. https://doi.org/10.1038/cddis.2015.327

[28] Deuse, T., Stubbendorff, M., Tang-Quan, K., Phillips, N., Kay, M.A., Eiermann, T., *et al.* (2011) Immunogenicity and Immunomodulatory Properties of Umbilical Cord Lining Mesenchymal Stem Cells. *Cell Transplantation*, **20**, 655-667. https://doi.org/10.3727/096368910x536473

[29] Martinez, E.C., Lilyanna, S., Wang, J. and Phan, T.T. (2013) Grafts Enriched with Subamnion-Cord-Lining Mesenchymal Stem Cell Angiogenic Spheroids Induce Post-Ischemic Myocardial Revascularization and Preserve Cardiac Function in Failing Rat Hearts. *Stem Cells and Development*, **22**, 3087-3099. https://doi.org/10.1089/scd.2013.0119

[30] McKinnon, R.D., Matsui, T., Dubois-Dalcq, M. and Aaronsont, S.A. (1990) FGF Modulates the PDGF-Driven Pathway of Oligodendrocyte Development. *Neuron*, **5**, 603-614. https://doi.org/10.1016/0896-6273(90)90215-2

[31] Olofsson, B., Pajusola, K., Kaipainen, A., von Euler, G., Joukov, V., Saksela, O., *et al.* (1996) Vascular Endothelial Growth Factor B, a Novel Growth Factor for Endothelial Cells. *Proceedings of the National Academy of Sciences*, **93**, 2576-2581. https://doi.org/10.1073/pnas.93.6.2576

[32] Cheong, H.H., Masilamani, J., Chan, C.Y.E., Chan, S.Y. and Phan, T.T. (2013) Metabolically Functional Hepatocyte-Like Cells from Human Umbilical Cord Lining Epithelial Cells. *ASSAY and Drug Development Technologies*, **11**, 130-138. https://doi.org/10.1089/adt.2011.444

[33] Friedenstein, A.J., *et al.* (1976) Multipotent Stromal Cells of Bone Marrow Origin: Cloning *in Vitro* and Retransplantation *in Vivo*. *Transplantation*, **17**, 331-340.

[34] Caplan, A.I. (1991) Mesenchymal Stem Cells. *Journal of Orthopaedic Research*, **9**, 641-650. https://doi.org/10.1002/jor.1100090504

[35] Dutra Alves, N.S., Reigado, G.R., Santos, M., Caldeira, I.D.S., Hernandes, H.d.S., Freitas-Marchi, B.L., *et al.* (2025) Advances in Regenerative Medicine-Based Approaches for Skin Regeneration and Rejuvenation. *Frontiers in Bioengineering and Biotechnology*, **13**, Article 1527854. https://doi.org/10.3389/fbioe.2025.1527854

[36] Lilyanna, S., Martinez, E.C., Vu, T.D., Ling, L.H., Gan, S.U., Tan, A.L., *et al.* (2013) Cord Lining-Mesenchymal Stem Cells Graft Supplemented with an Omental Flap Induces Myocardial Revascularization and Ameliorates Cardiac Dysfunction in a Rat Model of Chronic Ischemic Heart Failure. *Tissue Engineering Part A*, **19**, 1303-1315. https://doi.org/10.1089/ten.tea.2012.0407

[37] Maličev, E. and Jazbec, K. (2024) An Overview of Mesenchymal Stem Cell Heterogeneity and Concentration. *Pharmaceuticals*, **17**, Article 350. https://doi.org/10.3390/ph17030350

[38] In't Anker, P.S., Scherjon, S.A., Kleijburg-van der Keur, C., Noort, W.A., Claas, F.H.J., Willemze, R., *et al.* (2004) Amniotic Fluid as a Novel Source of Mesenchymal Stem Cells for Therapeutic Transplantation. *Blood*, **102**, 1548-1549. https://doi.org/10.1182/blood-2003-04-1291